Available online at www.sciencedirect.com
ScienceDirect
Geochimica et Cosmochimica Acta 70 (2006) 5323–5335
Geochimica
www.elsevier.com/locate/gca

Carbon isotopic fractionation by the marine diatom *Phaeodactylum tricornutum* under nutrient- and light-limited growth conditions

Nicolas Cassar [a], Edward A. Laws [b,*], Brian N. Popp [c]

[a] *Department of Geosciences, Princeton University, Princeton, NJ 08544, USA*
[b] *Department of Oceanography and Coastal Sciences, School of the Coast and Environment, Louisiana State University, Baton Rouge, LA 70803, USA*
[c] *Department of Geology and Geophysics, School of Ocean and Earth Sciences and Technology, University of Hawaii, Honolulu, HI 96822, USA*

Received 11 April 2006; accepted in revised form 14 August 2006

Abstract

A theoretical model was developed to explain the characteristics of carbon isotopic fractionation (ε_P) by the marine diatom *Phaeodactylum tricornutum* under nutrient- and light-limited growth conditions. The model takes into consideration active transport and diffusion of inorganic carbon through the cell membrane and chloroplast membrane and the energetic tradeoff between production of Rubisco and operation of a carbon-concentrating mechanism to achieve a given growth rate. The model is able to explain 88% of the variance in experimental ε_p data reported in this study and in previous work and is able to account for the observed pattern of Rubisco activity in nitrate-limited chemostats. Two important implications of the model include the fact that ε_p is not a unique function of the ratio of growth rate to external CO_2 concentration (as opposed to the predictions of several previous models) and that changes in light-limited and nutrient-limited growth rates have opposite effects on the fraction of CO_2 taken up by the chloroplast that is lost to diffusion and hence on certain patterns of carbon isotopic fractionation.

1. Introduction

One of the principal factors that has motivated the study of marine photosynthetic carbon isotope fractionation is the use of the isotopic record of sedimentary organic matter as a paleoceanographic proxy for CO_2 (e.g., Popp et al., 1997; Laws et al., 2002). However, a multitude of confounding factors can affect the relationship between photosynthetic carbon isotope fractionation (ε_p) and CO_2 (Laws et al., 2002). A quantitative understanding of the relationship between these confounding factors and ε_p is necessary before the sedimentary stable carbon isotopic record can be used with confidence for paleo-CO_2 reconstruction.

Based on inorganic carbon isotope mass balance, Sharkey and Berry (1985) and Francois et al. (1993) showed that the overall carbon isotopic signature of a phototroph can be expressed as a function of the carbon source, the transport mechanism from the medium to the site of carboxylation, the proportion of the intracellular inorganic carbon that leaks out of the cell before being fixed, and the carboxylating enzyme(s):

$$\varepsilon_p = \varepsilon_{up} + f_{eff}(\varepsilon_{fix} - \varepsilon_{diff}) \quad (1)$$

where

$$\varepsilon_p = \frac{\delta^{13}C_{CO_2} - \delta^{13}C_p}{1 + \frac{\delta^{13}C_p}{1000}} \quad (2)$$

and

$$\delta^{13}C = 1000\left(\frac{(^{13}C/^{12}C)_{sample}}{(^{13}C/^{12}C)_{PDB}} - 1\right) \quad (3)$$

where $\delta^{13}C_{CO_2}$ and $\delta^{13}C_p$ are the $\delta^{13}C$ of the aqueous CO_2 and phytoplankton carbon, respectively (Francois et al., 1993). ε_{up}, ε_{diff}, and ε_{fix} are the isotopic discriminations associated with the processes that bring inorganic carbon

* Corresponding author. Fax: +1 225 578 5328.
E-mail address: edlaws@lsu.edu (E.A. Laws).

0016-7037/$ - see front matter © 2006 Elsevier Inc. All rights reserved.
doi:10.1016/j.gca.2006.08.024

through the plasmalemma into the cell, diffusion back into the surrounding medium, and enzymatic carboxylation, respectively, and f_{eff} is the ratio of gross CO_2 diffusion out of the cell to gross inorganic carbon uptake. Assuming that CO_2 leaves the cell by passive diffusion, it is straightforward to show (Laws et al., 1997) that ε_p is controlled by the quotient of growth rate (μ, with units of d^{-1}) and the concentration of CO_2 at the interior surface of the plasmalemma (C_i, with units of μM) through the following equation:

$$\varepsilon_p = \varepsilon_{up} + \frac{\varepsilon_{fix} - \varepsilon_{diff}}{1 + \frac{\mu C}{PC_i}} \quad (4)$$

where P (L d^{-1} $cell^{-1}$) is the permeability of the plasmalemma to CO_2, C (μmol $cell^{-1}$) is the organic carbon content of the cell, and C_i is the concentration of CO_2 that diffuses out of the plasmalemma. If inorganic carbon enters the cell entirely by passive diffusion of CO_2, then $\mu C = P(C_e - C_i)$ and Eq. (4) can be rearranged to give (Laws et al., 1995)

$$\varepsilon_p = \varepsilon_{up} + (\varepsilon_{fix} - \varepsilon_{diff})\left(1 - \frac{\mu C}{PC_e}\right) \quad (5)$$

where C_e (μM) is the CO_2 concentration in the external medium. The quotient of μ and C_e has been considered a measure of the inorganic carbon demand/supply ratio. This demand/supply model assumes phytoplankton physiology to be static and passive, in which case the dependence of ε_p on μ/C_e is linear. However, ε_p has been shown to become increasingly insensitive to μ/C_e as this quotient increases, resulting in a non-linear relationship that can be explained by active uptake of inorganic carbon (Laws et al., 1997; Keller and Morel, 1999). The insensitivity of ε_p to μ/C_e at high values of the latter compromises the use of the sedimentary record as a proxy for paleo-CO_2 if CO_2 concentrations were low (i.e., μ/C_e was high) when the organic matter was formed.

Further confounding the interpretation of the sedimentary $\delta^{13}C$ record has been the observation that even for a single species the relationship between ε_p and μ/C_e may not be unique. Riebesell et al. (2000), for example, report differences in patterns of carbon fractionation for *Phaeodactylum tricornutum* grown under nitrate and light-limited conditions. They speculate that these differences may "reflect higher rates of active carbon uptake [in N-limited chemostats], fueled by elevated ATP/e^- ratios."

For a given species there is now general agreement that a variety of factors can affect carbon fractionation, including growth rate, the factor limiting growth, CO_2 concentration, and the presence or absence of various forms of carbon concentrating mechanisms (CCMs). Active uptake of bicarbonate (HCO_3^-) and CO_2 through the cell membrane, active transport of inorganic carbon (Sharkey and Berry, 1985; Badger, 1987; Johnston, 1991) from the cellular membrane to the chloroplasts, and active, unidirectional conversion of carbon dioxide to bicarbonate by a carbonic anhydrase-like mechanism are putative CCMs. Most theoretical studies have attributed changes in patterns of carbon isotope fractionation (e.g., ε_p vs. μ/CO_2) to differences in CCM activity and the ratio of diffusion to active transport of inorganic carbon (Laws et al., 1997; Keller and Morel, 1999). At some level of CO_2 deprivation, many marine phytoplankton species are capable of inducing CCM's in alleviating CO_2 limitation (Raven, 1997; Colman et al., 2002). The CCM's function is to elevate the CO_2 concentration in the vicinity of Rubisco above the concentration associated with passive diffusion in order to favor carboxylation versus oxidation and hence suppress photorespiration. At CO_2 levels less than roughly 10 μM, ε_p is greater than expected from a passive diffusion model (Laws et al., 1997) because the CO_2 concentration in the medium does not adequately represent the CO_2 concentration to which Rubisco is exposed. The increasing divergence of the empirical fractionation data from a passive diffusion model at high μ/C_e is very likely caused by the induction of CCMs (Laws et al., 2002).

The focus of current carbon isotope fractionation models on the influence of gross inorganic carbon influx across the plasmalemma (e.g., Keller and Morel (1999), Laws et al. (1997)) is motivated in part by the paucity of information on C_i (Eq. (4)) and its response to changes in growth conditions. However, this focus on gross uptake fails to consider the potential influence of variations of the intracellular CO_2 concentration on carbon fixation kinetics as influenced by Rubisco abundance and the concentration of CO_2 at the site of carboxylation. Changes in carbon fixation kinetics, which have hitherto received little attention in the context of carbon fractionation (but see Thoms et al., 2001), may respond to variations in growth conditions and consequently influence carbon isotope fractionation during photosynthesis.

To circumvent the catalytic inefficiency of their main carbon-fixing enzyme and alleviate CO_2 limitation, aquatic photoautotrophs can (1) actively increase the CO_2 available for photosynthesis through CCM activity and/or (2) vary the cellular abundance of Rubisco in response to changes in the intracellular inorganic carbon concentration. (We do not discuss the C_4 pathway (Reinfelder et al., 2000; Reinfelder et al., 2004) because we did not find evidence that it is important in the diatom under study (Cassar, 2003)). These two adaptive strategies should have opposite effects on the intracellular inorganic carbon concentration and hence on photosynthetic carbon isotope fractionation. As the external CO_2 decreases, CCM activity may increase C_i relative to the concentration associated with purely diffusive uptake and therefore cause fractionation to be greater than expected from Eq. (5). The alternative strategy is to increase Rubisco abundance to compensate for the decrease in intracellular inorganic carbon concentration, drawing down the intracellular CO_2 concentration even further and reducing f_{eff} and hence ε_p (Eq. (1)). Up-regulation of Rubisco abundance through nitrogen reallocation in response to sub-ambient CO_2 concentrations is well documented in terrestrial phototrophs (Sage, 1990, 1994; Anderson et al., 2001). In either case, CO_2 leakage is required to effect discrimination.

In this study, we extend an earlier model of carbon fractionation (Laws et al., 1997) to include the effects of active transport through the chloroplast membrane and the response of Rubisco kinetics to variations in CO_2 availability and growth rate in the marine diatom *P. tricornutum* Bohlin. We compare the predictions of the model with data obtained under both light- and nutrient-limited growth conditions and with two clones of *P. tricornutum*. We show that a simple model of carbon transport and fixation can explain patterns of carbon fractionation under light- and nutrient-limited growth conditions and that the predictions of the model are consistent with experimental data on Rubisco kinetics for nitrate-limited cultures.

2. Materials and methods

2.1. Continuous culture experiments and carboxylase assays

The marine diatom *P. tricornutum* Bohlin clone CCMP 1327 was grown at a temperature of 22.0 ± 0.1 °C and a salinity of 33‰ in a nitrate- or phosphate-limited continuous culture system identical to that described by Laws et al. (1995). Light was provided by a bank of daylight fluorescent lamps at a continuous irradiance of 21.6 mol quanta $m^{-2}\,d^{-1}$ (400–700 nm radiation). The partial pressure of CO_2 in the gas used to aerate the growth chamber was controlled using mass-flow controllers to adjust the flow rates of tank CO_2 (2.06% CO_2 in air) and CO_2-free air. Sampling for isotopic analysis of the particulate carbon in the growth chamber was not begun until the culture had completed at least four doublings at a given growth rate and the $\delta^{13}C$ of the DIC in the growth chamber had stabilized to ±0.1‰ from day to day. Once isotopic equilibrium was reached in the chemostats, samples were taken for chemistry and stable isotope measurements. Stable carbon isotope measurements were made following the procedures in Laws et al. (1995) and Cassar et al. (2002).

Aliquots (100 mL) for enzymatic analysis were filtered onto GF/F filters. The filters were homogenized in a buffer at 0 °C for 20 min with a glass potter for enzyme resuspension. The Rubisco assays were adapted from the method of Lavergne et al. (1979a,b), Descolas-Gros and Oriol (1992) and Reinfelder et al. (2000). Briefly, the enzymatic activity was measured by following the *in vitro* incorporation of radioactive bicarbonate into organic compounds in the presence of substrates chosen to maximize Rubisco activity. Enzyme extractions were performed in bicine buffers (50 mM) at pH 8. The extraction solutions contained $NaHCO_3$ (10 mM), glycerol (1.5 M), EDTA (1 mM), $MgCl_2$ (10 mM), DTT (5 mM), and bovine serum albumin (5 mg/L). All assays were performed at 25 ± 0.2 °C for 30 min in a temperature-controlled water bath. Prior to the assays, the crude extracts were maintained at 25 ± 0.2 °C for 30 min in the absence of the substrate. Reactions were initialized by the addition of ribulose bisphosphate (Rubp) and radiolabeled sodium bicarbonate. Carboxylase assays were performed in triplicates. The average of duplicate blanks was removed from the total carboxylase activity measured. Blanks were identical to the normal assays except for the absence of Rubp. Reactions for all assays were stopped with the addition of 6 N HCl. Samples were then evaporated to dryness, and 1 ml of deionized water was added with 10 ml of the scintillation cocktail Aquasol-2. The radioactive signal was then measured in a Packard Tri-Carb 4640 scintillation counter. Carboxylase activities were normalized to cell concentrations and expressed in units of nmol carbon fixed $cell^{-1}\,h^{-1}$.

3. Theory

The conceptual model is shown in Fig. 1. Inorganic carbon enters the cell via active transport through the plasma membrane at a rate F_1 and then through the membrane of the chloroplast at a rate F_2. CO_2 diffuses out of the chloroplast at a net rate F_3 and out of the cell at a net rate F_4. CO_2 is fixed within the chloroplast at a rate μC. From simple mass balance it follows that $F_1 + F_3 = F_2 + F_4$ and $F_2 = F_3 + \mu C$. The net diffusional fluxes F_3 and F_4 are assumed to be described by the equations $F_3 = P'(C_c - C_i)$ and $F_4 = P(C_i - C_e)$, where P and P' are the permeabilities of the plasma membrane and chloroplast membrane, respectively, C_e is the concentration of CO_2 in the external medium, C_i is the concentration of CO_2 in the cytosol, and C_c is the concentration of CO_2 within the chloroplast. It follows that $F_1 = P(C_i - C_e) + \mu C$ and $F_2 = P'(C_c - C_i) + \mu C$. In developing a model of the energetics of active transport, we consider two alternative models. In the first case we assume that $C_i > C_e$, and in the second we assume that $C_i \leqslant C_e$. In both cases we assume that $C_c > C_i$, i.e., that a CCM increases the concentration of CO_2 at the site of carboxylation.

3.1. First model

In the first model active transport through the plasmalemma occurs against a concentration gradient. Following Laws et al. (1997), we assume that the energetic costs of F_1 and F_2 are directly proportional to the associated differences in CO_2 concentrations, i.e., $C_i - C_e$ and $C_c - C_i$, respectively. The concentration of CO_2 within the chloroplast, C_c, is assumed to reflect an energetic tradeoff between the costs associated with the active transport system and the costs associated with producing and maintaining an amount of Rubisco sufficient to fix carbon at a rate μC at the concentration C_c of CO_2 within the chloroplast. Carbon fixation is assumed to follow Michaelis–Menten kinetics, i.e.,

$$\mu C = \frac{V_m C_c}{K_m + C_c} \tag{6}$$

where V_m is the substrate-saturated fixation rate and K_m is the concentration of C_c at which the fixation rate is half V_m. It is reasonable to assume that the concentration of Rubisco is proportional to V_m and that the energetic cost

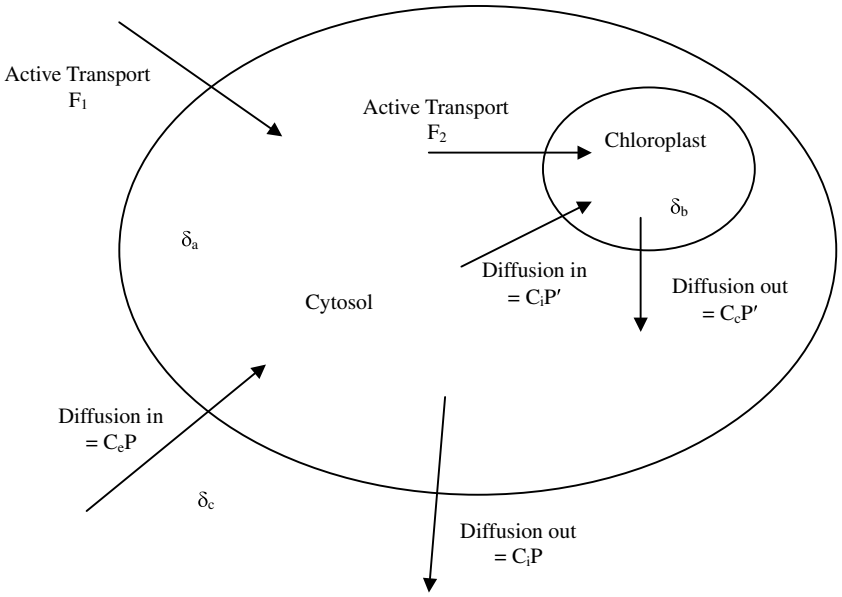

Fig. 1. Conceptual model of carbon fluxes through cell membrane and chloroplast membrane.

of maintaining this amount of Rubisco is proportional to the Rubisco concentration. From Eq. (6) it follows that $V_m = \mu C(1 + K_m/C_c)$. The overall energetic cost, E, of actively transporting CO_2 to Rubisco and fixing the CO_2 is therefore given by the equation

$$E = (P(C_i - C_e) + \mu C)B_1(C_i - C_e) + (P'(C_c - C_i) + \mu C) \times B_2(C_c - C_i) + B_3\mu C\left(1 + \frac{K_m}{C_c}\right) \quad (7)$$

where B_1, B_2, and B_3 are constants that reflect the energetic costs associated with active transport of inorganic carbon across the plasma membrane, active transport of inorganic carbon across the chloroplast membrane, and maintenance of Rubisco, respectively.

We now assume that the cell adjusts C_i and C_c so as to minimize E. Differentiating Eq. (7) with respect to C_i and C_c and setting the partial derivatives equal to zero gives the following two equations

$$\frac{\partial E}{\partial C_i} = 2PB_1(C_i - C_e) + \mu C(B_1 - B_2) - 2P'B_2(C_c - C_i) = 0 \quad (8)$$

$$\frac{\partial E}{\partial C_c} = 2P'B_2(C_c - C_i) + \mu CB_2 - \frac{B_3\mu CK_m}{C_c^2} = 0 \quad (9)$$

In order for these two equations to define a minimum it must be true that both $\frac{\partial^2 E}{\partial C_i^2}$ and $\frac{\partial^2 E}{\partial C_c^2}$ are positive and that $(\frac{\partial^2 E}{\partial C_i \partial C_c})^2 - (\frac{\partial^2 E}{\partial C_i^2})(\frac{\partial^2 E}{\partial C_c^2}) < 0$ (Laws, 1997). From Eqs. (8) and (9) it follows that $\frac{\partial^2 E}{\partial C_i^2} = 2(PB_1 + P'B_2)$, $\frac{\partial^2 E}{\partial C_c^2} = 2P'B_2 + \frac{2B_3\mu CK_m}{C_c^3}$, and $\frac{\partial^2 E}{\partial C_i \partial C_c} = -2P'B_2$. It is therefore obvious that both $\frac{\partial^2 E}{\partial C_i^2}$ and $\frac{\partial^2 E}{\partial C_c^2}$ are positive, and with a little algebra it follows that $(\frac{\partial^2 E}{\partial C_i \partial C_c})^2 - (\frac{\partial^2 E}{\partial C_i^2})(\frac{\partial^2 E}{\partial C_c^2}) = -2(PB_1 + P'B_2)\frac{2B_3\mu CK_m}{C_c^3} - 4PP'B_1B_2 < 0$. Hence, the values of C_i and C_c that solve Eqs. (8) and (9) will determine the minimum energetic cost of transporting and fixing CO_2.

With some algebraic manipulation (see Appendix A) it is straightforward to show that the value of C_c that solves Eqs. (8) and (9) is the positive real root of the cubic equation

$$C_c^3 + C_c^2\left(\alpha\mu\left(\frac{1+f}{2f}\right) - C_e\right) - \frac{\mu\alpha\chi^2}{2f\beta}(\beta + (1-\beta)f) = 0 \quad (10)$$

where $\alpha = \frac{C}{P}$, $\beta = \frac{B_1}{B_1+B_2}$, $\chi = \sqrt{\frac{B_3}{B_2}K_m}$, and $f = \frac{P'}{P}$. Given the value of C_c, the solution for C_i is given by the equation

$$C_i = \frac{C_c(2f)(1-\beta) + 2\beta C_e + \alpha\mu(1-2\beta)}{2(f(1-\beta)+\beta)} \quad (11)$$

3.2. Second model

In the second model ($C_i \leqslant C_e$) the cost of active transport through the plasmalemma is assumed to be negligible (because $C_i \leqslant C_e$) compared to the cost of active transport through the chloroplast membrane, which occurs against a concentration gradient. In that case Eq. (7) reduces to

$$E = (P'(C_c - C_i) + \mu C)B_2(C_c - C_i) + B_3\mu C\left(1 + \frac{K_m}{C_c}\right) \quad (12)$$

The right-hand side of Eq. (12) is minimized by making C_i as large as possible. Given the assumption that $C_i \leqslant C_e$, this clearly implies that $C_i = C_e$. Setting $C_i = C_e$, differentiating Eq. (12) with respect to C_c, and setting the partial derivative equal to zero gives

$$\frac{\partial E}{\partial C_c} = 2P'B_2(C_c - C_e) + \mu CB_2 - \frac{B_3\mu CK_m}{C_c^2} = 0 \quad (13)$$

Manipulation of Eq. (13) (see Appendix A) leads to the following equation:

$$C_c^3 + \left(\frac{\alpha\mu}{2f} - C_e\right)C_c^2 - \frac{\chi^2\alpha\mu}{2f} = 0 \quad (14)$$

In summary, Eqs. (10), (11) determine C_i and C_c when active transport across the plasmalemma occurs against a concentration gradient (model 1). Otherwise $C_i = C_e$ (model 2), and C_c is determined from Eq. (14). An important point about the first and second model is the fact that they do not converge when $C_i = C_e$. Although Eqs. (7) and (12) are identical when $C_i = C_e$, the fact that two functions are equal by no means implies that their derivatives are equal, and of course it is the derivatives of Eqs. (7) and (12) that determine the behavior of the two models.

3.3. Light-limited growth

Riebesell et al. (2000) have argued that differences they noted in carbon isotopic fractionation patterns between *P. tricornutum* clone CCAP 1052/1A and clone CCMP 1327 (Laws et al., 1997) may reflect the fact that they grew the former clone under light-limited conditions, while Laws et al. (1997) grew clone CCMP 1327 in a nitrate-limited chemostat. They point out (p. 300, 301) that ATP and NADPH "must be delivered in a ratio (ATP/e^-) which matches the requirement to synthesize biomass... An increase in the proportion of non-linear to linear electron transport increases the ATP/e^- ratio and thus the amount of chemical energy available for processes such as active carbon transport." They go on to point out (p. 301), "The relative contribution of non-linear electron flow to steady-state photosynthesis and its regulation under variable environmental conditions is poorly quantified."

In analyzing our data, we assumed that Riebesell et al.'s (2000) postulates about the ATP/e^- ratio were basically correct. Under light-limited conditions, they argue that the ATP/e^- ratio is likely to be lower than under nitrate-limited conditions and that the amount of chemical energy available for processes such as active carbon transport therefore reduced. To incorporate these arguments into our model in a simple way, we assumed that for *P. tricornutum* growth rate was a power function of irradiance, i.e., $\mu \propto I^{1/n}$, where n is a small integer (Terry et al., 1983). Hence, $I \propto \mu^n$. We then postulated that under light-limited conditions the effective metabolic cost of active transport relative to carbon fixation would be inversely proportional to irradiance, since active transport must compete with chemical synthesis for ATP that is generated under light-limited conditions in more-or-less constant proportion to NADPH. It follows that under light-limited conditions, $B_1 \to B_1/\mu^n$, and $B_2 \to B_2/\mu^n$. Of the four parameters α, β, χ, and f, this assumption affects only χ. Under light-limited conditions, $\chi \to \mu^{n/2}\,\chi'$. The result is that Eq. (10) becomes

$$C_c^3 + C_c^2\left(\alpha\mu\left(\frac{1+f}{2f}\right) - C_e\right) - \frac{\mu^{n+1}\alpha(\chi')^2}{2f\beta}(\beta + (1-\beta)f) = 0 \quad (15)$$

and Eq. (14) becomes

$$C_c^3 + \left(\frac{\alpha\mu}{2f} - C_e\right)C_c^2 - \frac{(\chi')^2\alpha\mu^{n+1}}{2f} = 0 \quad (16)$$

3.4. Constraints on parameter values

The solutions for C_i and C_c under both nutrient- and light-limited growth conditions require specification of six parameters, α, f, and β, χ', and n. The value of α can be estimated from information in the literature. The cell carbon content of *P. tricornutum* varies between roughly 5 and 18 pg cell^{-1} with a mean of 10.0 ± 3.1 pg cell^{-1} or $8.3\times10^{-7} \pm 2.6\times10^{-7}$ μmol cell^{-1} (Riebesell et al., 2000). Based on the work of Rau et al. (1997), we estimated P to be 5×10^{-5} m s^{-1}. Multiplying P by the surface area of *P. tricornutum* (174 μm^2, (Laws et al., 1997)) gives $P = 7.5\times10^{-7}$ L d^{-1} cell^{-1}. The value of $\alpha = C/P = 1.1$ μM d. Terry et al. (1983) studied the light-limited growth of two strains of *P. tricornutum* and found that growth rate varied as irradiance raised to the 0.26 power. According to our model, this would imply that $n = 1/0.26 = 3.8$. We rounded off n to 4. We reasoned that under light-saturated conditions the two models should merge. This implies that $\chi = (\mu_{max})^2\chi'$, where μ_{max} is the maximum growth rate. Based on the information in Riebesell et al. (2000) and Terry et al. (1983), we estimated μ_{max} to be 2.3 d^{-1} under continuous irradiance at 22 °C. This implies $\chi = (2.3)^2\chi' = 5.3\ \chi'$. With this constraint equation and α and n determined, we were left with three unconstrained variables, f, β, and χ (or χ'). The parameters f and β are dimensionless. The value of β clearly lies in the range zero to one. The chloroplast of diatoms is surrounded by a double-layered envelope and a double-layered endoplasmic reticulum, presumably reflecting the engulfment of a cyanobacterium by a eukaryotic host cell (Martin et al., 2002; Falkowski et al., 2004; Tanaka et al., 2005). Furthermore, the surface area of the chloroplast is less than that of the cell (Fawley, 1984). It is therefore reasonable to assume that f will also lie in the range zero to one. An approximate lower bound on χ can be obtained based on the assumption that $C_c > C_i$. From Eq. (9) it follows that

$$C_c - C_i = \frac{\mu\alpha}{2f}\left(\frac{\chi^2}{C_c^2} - 1\right) \quad (17)$$

Thus χ must be larger than C_c for the results of either model to be consistent with the assumption that active transport into the chloroplast occurs against a concentration gradient. The K_m for Rubisco has been estimated to lie in the range 20 to 70 μM (Badger et al., 1998). Assuming that C_c is comparable to K_m, the lower bound on χ is roughly 20 to 70 μM. In the case of the first model, an upper bound on β may likewise be obtained based on the assumption that active transport through the plasmalemma occurs against a concentration gradient. Rearranging Eq. (8) gives

$$C_i - C_e = \frac{fB_2(C_c - C_i)}{B_1} - \frac{\mu\alpha(B_1 - B_2)}{2B_1}$$
$$= \frac{1-\beta}{\beta}\frac{\mu\alpha}{2}\left(\frac{\chi^2}{C_c^2} - 1\right) - \frac{\mu\alpha}{2}\left(1 - \frac{1-\beta}{\beta}\right) \quad (18)$$
$$= \frac{\mu\alpha}{2}\left(\frac{(1-\beta)}{\beta}\frac{\chi^2}{C_c^2} - 1\right)$$

Since the lower bound on $\frac{\chi^2}{C_c^2}$ is 1.0 (Eq. (17)), it follows that C_i will be greater than C_e if $\frac{(1-\beta)}{\beta} \geqslant 1$. This condition is ensured if $\beta \leqslant 0.5$. Parameter values were chosen so as to minimize the sum of the squared deviations of the experimental and calculated combined light- and nutrient-limited experimental ε_p data reported here and by (Riebesell et al., 2000, Table 1) and (Laws et al., 1997, Table 1).

3.5. Derivation of equation for ε_p

Given the assumptions of the model, an equation somewhat more complex than Eq. (1) must be used to calculate ε_p. The relevant mass balance equations are as follows:

$$(P(C_i - C_e) + \mu C)(\delta_{source} - \varepsilon_t) + C_e P(\delta_c - \varepsilon_t) + C_c P'(\delta_b - \varepsilon_t) = C_i P'(\delta_a - \varepsilon_t) + (P'(C_c - C_i) + \mu C)(\delta_a - \varepsilon_t) + C_i P(\delta_a - \varepsilon_t) \quad (19)$$

$$C_i P'(\delta_a - \varepsilon_t) + (P'(C_c - C_i) + \mu C)(\delta_a - \varepsilon_t) = C_c P'(\delta_b - \varepsilon_t) + \mu C(\delta_b - \varepsilon_{fix}) \quad (20)$$

The first, second, and third terms on the left-hand side of Eq. (19) describe input of inorganic carbon to the cytosol via active transport from the external medium, diffusion of CO_2 from the external medium, and diffusion of CO_2 from the chloroplast, respectively. The first, second, and third terms on the right-hand side of Eq. (19) describe diffusion of CO_2 from the cytosol through the chloroplast membrane, active transport of CO_2 from the cytosol through the chloroplast membrane, and diffusion of CO_2 out of the cell, respectively. The first and second terms on the left-hand side of Eq. (20) describe diffusion and active transport, respectively, of CO_2 from the cytosol through the chloroplast membrane. The first and second terms on the right-hand side of Eq. (20) describe diffusion of CO_2 out of the chloroplast and carbon fixation, respectively. Fractionation associated with diffusion and active transport is assumed to be small (~1‰) and equal to ε_t. Fractionation associated with carbon fixation equals ε_{fix} and is assumed to be 27‰ (see review by Goericke et al., 1994). δ_c, δ_a, and δ_b are the $\delta^{13}C$ of the CO_2 in the external medium, cytosol, and chloroplast, respectively. The $\delta^{13}C$ of the carbon actively transported from the external medium equals δ_{source}. Through algebraic manipulation (see Appendix A), $\delta_a - \varepsilon_t$ can be eliminated from Eqs. (19), (20) and an expression obtained for δ_b. The photosynthetically fixed carbon will have a $\delta^{13}C$ of $\delta_b - \varepsilon_{fix}$, which by convention is equated to $\delta_c - \varepsilon_p$. The expression for ε_p is

$$\varepsilon_p = (\delta_c - \delta_{source})\gamma(1 - \theta_a) + \theta_a\theta_b(\varepsilon_{fix} - \varepsilon_t) + \varepsilon_t \quad (21)$$

where θ_a ($= \frac{PC_i}{PC_i + \mu C}$) and θ_b ($= \frac{P'C_c}{P'C_c + \mu C}$) are the ratios of diffusional loss to gross uptake through the plasmalemma and chloroplast membrane, respectively, and γ ($= \frac{P(C_i - C_e) + \mu C}{\mu C}$) is the ratio of active transport through the plasmalemmma to carbon fixation. Eq. (21) is identical to Eq. (4) in Keller and Morel (1999) in the limit as $\theta_b \to 1$, i.e., in the limit as the chloroplast membrane is infinitely leaky, in which case δ_a and δ_b are identical.

4. Results

Phaeodactylum tricornutum clone CCMP 1327 lacks the ability to actively transport bicarbonate (Cassar et al., 2002). Clone CCAP 1052/1A has the ability to actively transport bicarbonate (Burkhardt et al., 1999, 2001), but it has a distinct preference for CO_2, which is taken up in roughly a 2:1 ratio to bicarbonate (Burkhardt et al., 2001). In parameterizing our model, we assumed that CO_2 was the form of inorganic carbon actively transported into the cells. We explore the implication of this assumption in the case of clone CCAP 1052/1A in the Discussion. Assuming active transport of CO_2, $\delta_{source} = \delta_c$, and $\varepsilon_p = \theta_a\theta_b(\varepsilon_{fix} - \varepsilon_t) + \varepsilon_t$.

Although model 1 has three adjustable parameters (β, f, and χ) and model 2 has only two (f and χ), model 2 gave a much better fit to the experimental data (Fig. 2). Model 1 accounted for 64% of the variance in the experimental ε_p values; model 2 accounted for 88%. The principal difference between the two models was the tendency of model 1 to overestimate fractionation under nutrient-limited conditions when the experimental ε_p were less than about 15‰. The ability of model 1 to describe the experimental data could be improved by increasing the value of β, but this resulted in violations of the assumption that $C_i > C_e$ (*vide supra*). Given the much better fit of model 2 to the experimental data, the remaining analysis was carried out using model 2.

The standard deviation of the difference between the calculated and measured ε_p values was 1.8‰ for model 2. Least squares values of f and χ were 0.050 ± 0.009, and 223 ± 56 μM, respectively, where the error bounds are standard deviations. The standard deviations of f and χ were calculated using the following Monte-Carlo approach. The measured ε_p values were noise corrupted using normally distributed random numbers with a mean of zero and a standard deviation of 1.8‰ and the least squares values of f and χ determined for the noise-corrupted dataset. This process was repeated 200 times. The standard deviations reported above are the standard deviations of the 200 f and χ values so calculated.

For both the light- and nutrient-limited datasets, there was a significant correlation between C_c and μ ($r = 0.98$ and 0.67, respectively) and a good correlation between C_c and C_e ($r = 0.78$) under nutrient limitation (Fig. 3). All of these correlations were significant at $p < 0.002$. There

Table 1
Parameters used in the model

Parameter	Definition	Units
α	C/P	1.1 μmol d L^{-1}
β	$B_1/(B_1+B_2)$	Dimensionless
χ	$\sqrt{\frac{B_3}{B_2}K_m}$	μmol L^{-1}
χ'	χ/μ_{max}^2	μmol d^2 L^{-1}
B_1	Constant proportional to the energetic cost associated with active transport of inorganic carbon across the plasma membrane	Energy cell d L μmol^{-2}
B_2	Constant proportional to the energetic cost associated with active transport of inorganic carbon across the chloroplast membrane	Energy cell d L μmol^{-2}
B_3	Constant proportional to the energetic cost associated with maintenance of Rubisco	Energy cell d μmol^{-1}
C	Carbon content of the cell	$\frac{10}{12}\times 10^{-6}$ μmol $cell^{-1}$
C_c	CO_2 concentration in the external medium	μmol L^{-1}
C_e	CO_2 concentration in the external medium	μmol L^{-1}
C_i	CO_2 concentration in the external medium	μmol L^{-1}
δ_a	$\delta^{13}C$ of the CO_2 in the cytosol	Dimensionless
δ_b	$\delta^{13}C$ of the CO_2 in the chloroplast	Dimensionless
δ_c	$\delta^{13}C$ of the CO_2 in the external medium	Dimensionless
δ_{source}	$\delta^{13}C$ of the carbon actively transported from the external medium	Dimensionless
ε_{diff}	Isotopic discrimination associated with diffusion of inorganic carbon into the medium surrounding the cell	Dimensionless (1‰)
ε_{fix}	Isotopic discrimination associated with enzymatic carboxylation	Dimensionless (27‰)
ε_p	Apparent fractionation between photosynthetically fixed carbon and CO_2 in the external medium	Dimensionless
ε_{up}	Isotopic discrimination associated with the process that brings inorganic carbon through the plasmalemma into the cell	Dimensionless
ε_t	Fractionation associated with diffusion and active transport	Dimensionless (1‰)
f	P'/P	Dimensionless
f_{eff}	Ratio of gross CO_2 diffusion out of the cell to gross inorganic carbon uptake	Dimensionless
F_1	Rate at which inorganic carbon enters the cell via active transport through the plasma membrane	μmol $cell^{-1}$ d^{-1}
F_2	Rate at which inorganic carbon enters the chloroplast via active transport from the cytosol	μmol $cell^{-1}$ d^{-1}
F_3	Net rate at which CO_2 diffuses out of the chloroplast	μmol $cell^{-1}$ d^{-1}
F_4	Net rate at which CO_2 diffuses out of the cell	μmol $cell^{-1}$ d^{-1}
γ	Ratio of active transport through the plasmalemma to net growth rate $=\frac{P(C_i-C_e)+\mu C}{\mu C}$	Dimensionless
K_m	Rubisco half-saturation constant	μmol L^{-1}
μ	Net growth rate of the cell	d^{-1}
μ'	Gross growth rate of the cell	d^{-1}
n	$I \propto \mu^n$ for light-limited growth	4 (dimensionless)
P	Permeability of the plasmalemma to CO_2	7.5×10^{-7} L d^{-1} $cell^{-1}$
P'	Permeability of the chloroplast membrane to CO_2	L d^{-1} $cell^{-1}$
θ_a	Ratio of CO_2 that leaks out of the cell to gross uptake through the plasmalemma $=\frac{C_iP}{\mu C+C_iP}$	Dimensionless
θ_b	Ratio of CO_2 that leaks out of the chloroplast to gross uptake by the chloroplast $=\frac{P'C_c}{P'C_c+\mu' C}$	Dimensionless
V_m	Rubisco substrate-saturated fixation rate	μmol $cell^{-1}$ d^{-1}

was no significant correlation ($p = 0.11$) between C_c and C_e under light-limited conditions.

An important characteristic of the new model is that there is no longer a unique relationship between μ/C_e and ε_p (Fig. 4). At a fixed μ/C_e ε_p is negatively correlated with growth rate under nutrient limitation (Fig. 4a) and positively correlated with growth rate under light limitation (Fig. 4b).

Based on our theoretical model we expected the measured Rubisco activities for clone CCMP 1327 to be directly proportional to $\mu(1 + K_m/C_c)$. This was the case for the nitrate-limited cultures (Fig. 5), although with only three data points the correlation is significant at only $p = 0.14$. Rubisco activities in the case of the two phosphate-limited cultures showed no correlation with $\mu(1 + K_m/C_c)$. These two cultures were both grown at a rate of 1.02 d^{-1} but at very low (0.4 μM) and very high (70.1 μM) C_e concentrations. The highest Rubisco activity was measured in the former culture.

5. Discussion

5.1. Important characteristics of new model

The model presented here differs from the earlier model of Laws et al. (1997) in two important respects. First, it

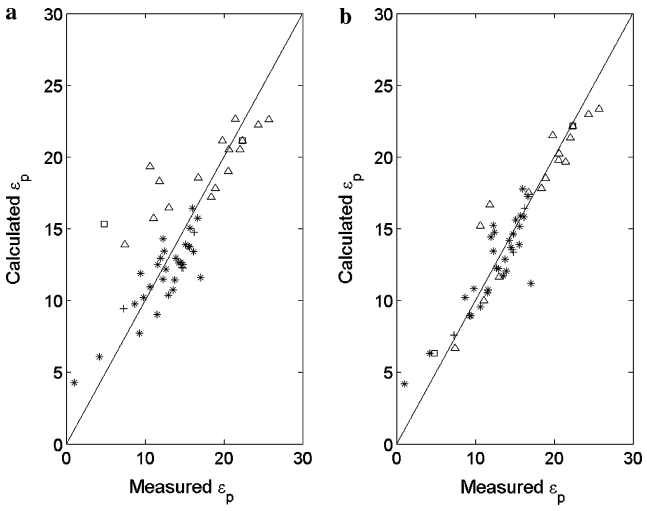

Fig. 2. Measured and calculated ε_p values for light-limited CCAP 1052/1A (∗), light-limited CCMP 1327 (+), nitrate-limited CCMP 1327 (△), and phosphate-limited CCMP 1327 (□) cultures of *P. tricornutum* using model 1 (a) and model 2 (b). Light-limited data are from (Riebesell et al., 2000, Table 1). Nutrient-limited data are from this study and (Laws et al., 1997, Table 1). For model 1 least squares parameters are $\beta = 0.5$, $f = 0.038$, and $\chi = 205$ μM. For model 2, $f = 0.05$ and $\chi = 223$ μM.

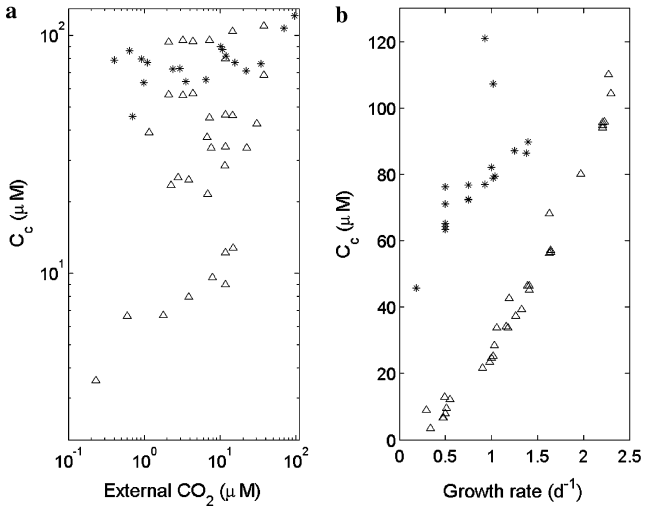

Fig. 3. Relationship between C_c and external CO_2 concentration (a) and between C_c and growth rate (b) for nutrient-limited (∗) and the light-limited (△) cultures of *P. tricornutum* using model 2.

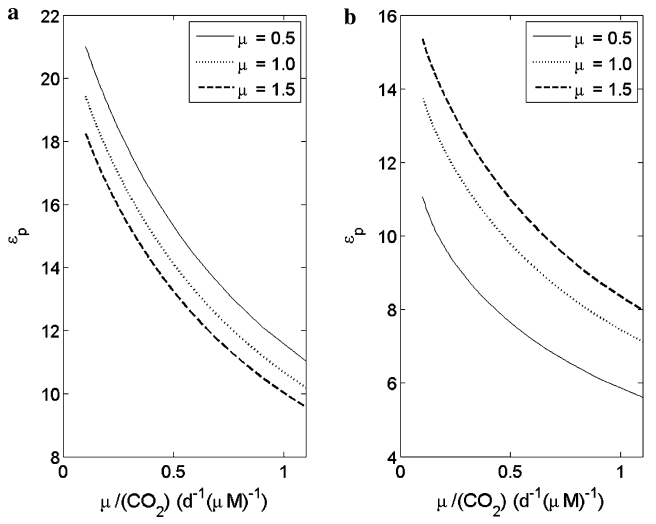

Fig. 4. Predicted relationship between ε_p and μ/CO_2 at growth rates of 0.5, 1.0, and 1.5 d^{-1} for nutrient-limited cultures (a) and light-limited cultures (b).

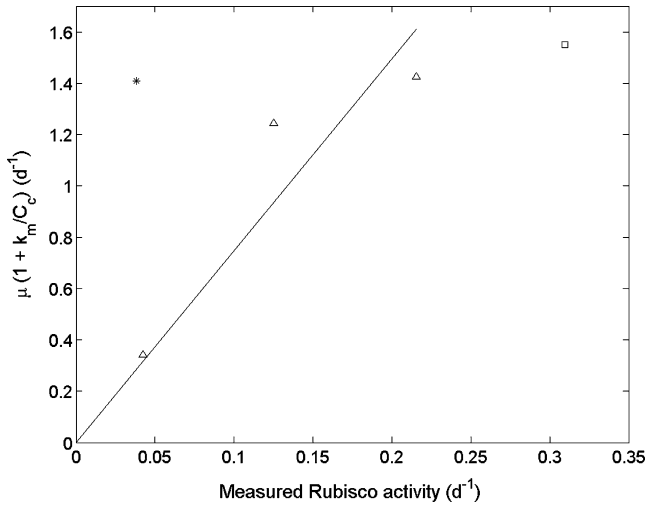

Fig. 5. Relationship between measured Rubisco activity and $\mu(1 + K_m/C_c)$ for nitrate-limited (△) and phosphate-limited cultures (□ and ∗). The straight line is a linear least squares fit to the nitrate-limited data. The K_m for Rubisco was assumed to be 41 μM (Badger et al., 1998).

takes into account diffusion of CO_2 from the chloroplast. If the chloroplast membrane were assumed to be infinitely permeable, C_i would be identical to C_c. However, the size and structure of the chloroplast (*vide supra*) result in $P' \ll P$. There is consequently a substantial difference between C_c and C_i. Second, the model takes into consideration the energetic cost associated with producing and maintaining Rubisco. If this cost were zero there would be no reason to concentrate CO_2 at the site of carboxylation, since the fixation rate required to sustain a given growth rate could be achieved by simply producing a sufficient quantity of Rubisco. Given the fact that Rubisco possesses an oxygenase activity, a caveat to this argument is that the CO_2 concentration at the active site must not fall below the concentration needed to permit net CO_2 fixation. Obviously, there is an energetic tradeoff between operation of a CCM on the one hand and Rubisco production and (potentially) operation of the photorespiratory carbon oxidation cycle on the other.

5.2. ε_p not a unique function of μ/CO_2

An important implication of the model is that ε_p is no longer a unique function of μ/CO_2. Furthermore, the fractionation to be expected at a given growth rate and CO_2 concentration must now be calculated by solving a cubic equation, although this can easily be done with modern software. The model appears to explain at least some of

the discrepancies in the literature concerning the effect of growth conditions on carbon fractionation. Many of the light-limited data reported by Riebesell et al. (2000), for example, were obtained from cultures grown over a range of CO_2 concentrations and at growth rates of approximately 0.5, 1.0, or 1.5 d^{-1}. As is apparent from Fig. 4, ε_p at a given μ/CO_2 could vary by roughly 2–5‰ within this range of growth rates.

5.3. Implications of parameter values

Several comments about the parameter values are in order. First, the value of f was, as expected, small compared to 1.0. The fact that $f \ll 1.0$ is probably the net result of several factors including the size, structure, and chemistry of the chloroplast. Since the rate of diffusion of gas through a membrane is directly proportional to the surface area of the membrane, the effective permeability of the chloroplast membrane was expected to be smaller than the permeability of the plasmalemma. Fawley (1984) studied the effects of irradiance and temperature on chloroplast length in batch cultures of *P. tricornutum*. He found that chloroplast length was positively correlated with temperature and negatively correlated with irradiance. Based on his results, we estimate the chloroplast length of *P. tricornutum* at 22 °C and an irradiance of 21.6 mol quanta m^{-2} d^{-1} to be 8–9 μm, which is roughly 60% of the length of the frustule (Popp et al., 1998). Assuming that the surface areas of the chloroplast and cell scale as the square of their linear dimensions, we would expect f to equal about 0.36. The fact that f is about seven times smaller suggests that the chloroplast membrane is relatively impermeable to CO_2 diffusion, a characteristic that facilitates maintenance of a large CO_2 differential between the chloroplast and cytosol. In addition, the chloroplast is a complex structure including, in the case of diatoms, a central lamella, pyrenoid, bulk stroma, bulk thylakoids, girdle lamella, and marginal stroma. Thoms et al. (2001, p. 306) point out, "Suppression of leakage is a major prerequisite for the construction of an efficient CCM. The chloroplast envelope, girdle lamella, and the pyrenoid appear to represent important diffusion barriers to CO_2. Also, CA [carbonic anhydrase] in the stroma converts a significant fraction of CO_2 not fixed by Rubisco to HCO_3^-, and acts as an additional (chemical) barrier against leakage of CO_2." In other words, the size, internal structure, and chemistry of chloroplasts combine to produce an organelle with an efficient barrier to diffusive loss of CO_2.

5.4. Nutrient-limited versus light-limited growth

Second, the fact that C_c is more closely correlated with growth rate than with C_e reflects in part the small value of f (i.e., P'/P). In Eq. (14), C_e appears only in the coefficient of the quadratic term in the polynomial. Although $\alpha\mu$ is small compared to C_e in most cases, $\alpha\mu/(2f)$ is 10 times bigger than $\alpha\mu$. Furthermore, the product of the three roots of the polynomial (Eq. (14)) must equal $\frac{\mu\alpha\gamma^2}{2f}$, which is a function of μ but independent of C_e. In other words, the product of the three roots of the polynomial is independent of C_e.

The absence of a unique relationship between ε_p and μ/C_e directly reflects the dependence C_c on μ and C_e. Since for model 2 $\theta_a = \frac{PC_i}{PC_i+\mu C} = \frac{1}{1+\frac{\gamma\mu}{C_e}}$, ε_p will be a unique function of μ/C_e as long as θ_b is either constant or also a function of μ/C_e. The fact that θ_b is neither constant nor a function of μ/C_e therefore has much to do with the behavior seen in Fig. 4. Under nutrient-limited conditions the ratio μ/C_c is positively correlated with μ, the result being that θ_b $(= \frac{P'C_e}{P'C_e+\mu C} = \frac{1}{1+\frac{\gamma\mu}{fC_e}})$ is negatively correlated with μ. Under light-limited conditions μ/C_c is negatively correlated with μ, the result being that θ_b is positively correlated with μ. The result of this behavior is that at a fixed μ/C_e, ε_p is negatively correlated with growth rate under nutrient limitation (Fig. 4a) and positively correlated with growth rate under light limitation (Fig. 4b). This analysis underscores the importance of CO_2 diffusion through the chloroplast membrane in determining the overall pattern of carbon fractionation. The difference in the relationships between μ/C_c and growth rate under nutrient and light limitation presumably reflects the availability of energy to operate a CCM (Riebesell et al., 2000). Under nutrient limitation there is adequate energy to concentrate CO_2 within the chloroplast even at low growth rates, the result being that C_c, although positively correlated with μ, varies by less than a factor of 3 (Fig. 3b). Under light limitation, the availability of energy to operate a CCM is related in a non-linear way to growth rate, the result being that C_c is much more sensitive to μ (Fig. 3b).

Our treatment of the effects of light limitation on the energetic costs of active transport versus chemical synthesis amounts to a parameterization of complex and poorly understood relationships. As a first approximation it seems reasonable to assume that the production of ATP via non-linear electron flow is directly proportional to irradiance. Given the non-linear relationship between growth rate and irradiance, our treatment of the energetic costs of active transport versus chemical synthesis under light-limited conditions probably captures the important features of the relationship. Given current understanding, a more complex treatment of this phenomenon is probably not warranted.

5.5. Rubisco biomass

Our estimates of Rubisco biomass are consistent with the model in the case of nitrate limitation but not in the case of phosphate limitation. Under phosphate-limited conditions, the physiological response of the cell to a change in growth rate or CO_2 concentration will differ from the response under nitrate limitation (Riebesell et al., 2000). Realizing that the production of Rubisco is associated with a large demand for nitrogen, it is plausible that an increase in growth rate will be accompanied by a greater increase in Rubisco biomass and a smaller increase in

C_c under phosphate limitation versus nitrate limitation. If true, however, such differences are not reflected by a change in ε_p (Fig. 2), and experimental confirmation of differences in physiological response is equivocal (see Table 1 in Raven et al., 2005).

5.6. Bicarbonate uptake

In the course of this study, we explored the use of two modifications of the model presented here. First, we explored the implications of assuming that some of the inorganic carbon taken up by clone CCAP 1052/1A was bicarbonate. Based on the work of Burkhardt et al. (2001), we assumed that bicarbonate was taken up at half the rate of CO_2 active transport. Since bicarbonate is isotopically heavy compared to CO_2 by about 9‰, the difference $\delta_c - \delta_{source}$ (Eq. (21)) should be about −3‰. With this adjustment and use of Eq. (21) to calculate ε_p, the least squares values of f and χ changed very little, and the goodness of fit to the ε_p data was not improved. The insensitivity of our results to this modification is due mainly to the fact that for clone CCAP 1052/1A the average value of $\gamma(1-\theta_a)$ was only 0.22. Hence, the correction factor averaged only −0.66‰, which is within the noise level of the data. Since $C_i = C_e$ in the second model, $\gamma = 1$, and θ_a is the ratio of gross uptake via diffusion to total gross uptake. The implication is that active transport accounted for an average of only 22% of gross inorganic carbon uptake for clone CCAP 1052/1A. It is perhaps also worth pointing out that by far the largest deviation of the CCAP 1052/1A ε_p data from the model predictions is associated with an observed ε_p of 17‰ (Fig. 2). The model predicts a fractionation of 11‰ in this case. This discrepancy is certainly not going to be explained by invoking bicarbonate transport.

5.7. Recycling of respiratory CO_2

The second modification was to allow for the addition of respired CO_2 to the cytosol (see Appendix A). Gross carbon fixation was assumed to occur at a rate μ', which exceeds the net rate μ, the difference being the respiration rate. In the case of model 2, taking account of respired CO_2 has no effect on the goodness of fit, but increases the least squares value of f by the ratio μ'/μ. This results from the fact that the parameters f and μ' always appear in the model equations in the ratio μ'/f. Hence, it is impossible to distinguish the effect of recycling respired CO_2 to the cytosol from an increase in the permeability of the chloroplast membrane. If there were some independent constraint on f, then incorporating respiration into the model might prove useful. The situation is very similar with model 1, although there is one term in Appendix A Eq. (A.10) ($\beta + f(1-\beta)$) where f occurs independently of μ'. We tried incorporating respiration into model 1, but the goodness of fit to the experimental ε_p data was not improved.

5.8. Implications for interpretation of isotopic records

Certainly one implication of this work is a reinforcement of the earlier conclusions of Popp et al. (1997), Riebesell et al. (2000), Laws et al. (2002), and others that carbon isotopic fractionation is affected by a number of environmental and physiological factors. Interpretation of the isotopic record in sediments will require that those factors be constrained before information on $\delta^{13}C$ in sedimentary organic matter can be related to paleo CO_2 concentrations. Compound-specific isotopic analysis may be used to isolate compounds associated with a particular species or taxonomic group. Most recent estimates of paleo CO_2 concentrations, for example, have been based on isotopic analysis of alkenones (e.g., Pagani et al., 2005), which are produced by a limited suite of haptophytes, in particular *Emiliania huxleyi* and *Gephyrocapsa oceanica* (Volkman et al., 1980a,b; Conte et al., 1994; Volkman et al., 1995). Consequently, if f and χ used in model 2 were known for alkenone-producing algae, paleo CO_2 reconstructions based on isotopic analysis of alkenones could be improved.

Acknowledgments

We thank John Raven, David M. Karl, Fred T. Mackenzie, Julie Granger, Robert R. Bidigare, and two anonymous reviewers for helpful comments, and Terri Rust for help in the laboratory. This work was supported in part by NSF Grant OCE-0424860 to E.A.L. This is SOEST Contribution No. 6821.

Associate editor: Juske Horita

Appendix A

Here, we provide the details of the derivations of Eqs. 10, 14, and 21. We begin with a slightly more general model by allowing for the introduction of respired CO_2 into the cytosol. We assume that the gross photosynthetic rate is $\mu' C$, which is greater than the net photosynthetic rate, μC. Under these conditions, the analogue of Eq. (7) is

$$E = (P(C_i - C_e) + \mu C)B_1(C_i - C_e) + (P'(C_c - C_i) + \mu' C)B_2(C_c - C_i) + B_3\mu' C\left(1 + \frac{K_m}{C_c}\right) \quad (A.1)$$

Note that there is no change to the term describing uptake of CO_2 from the external medium, since the respired carbon is assumed to be recycled within the cell. Differentiating Eq. (A.1) with respect to C_i and C_c gives

$$\frac{\partial E}{\partial C_i} = 2PB_1(C_i - C_e) + \mu C B_1 - \mu' C B_2 - 2P'B_2(C_c - C_i) = 0 \quad (A.2)$$

$$\frac{\partial E}{\partial C_c} = 2P'B_2(C_c - C_i) + \mu' C B_2 - \frac{B_3\mu' C K_m}{C_c^2} = 0 \quad (A.3)$$

Rearranging Eq. (A.3) gives

$$C_c - C_i = \frac{B_3\mu' CK_m}{2P'B_2C_c^2} - \frac{\mu' C}{2P'} \tag{A.4}$$

Rearranging Eq. (A.4) gives

$$C_i = C_c - \frac{B_3\mu' CK_m}{2P'B_2C_c^2} + \frac{\mu' C}{2P'} = C_c - \frac{\mu'\alpha\chi^2}{2fC_c^2} + \frac{\mu'\alpha}{2f} \tag{A.5}$$

Eq. (A.2) can be written as

$$(C_i - C_e) + \frac{\mu\alpha}{2} - \frac{\mu'\alpha}{2}\left(\frac{1-\beta}{\beta}\right) - f\frac{(1-\beta)}{\beta}(C_c - C_i) = 0 \tag{A.6}$$

Where α, β, and f are as previously defined. Substituting the right-hand side of Eq. (A.5) for C_i in Eq. (A.6) gives

$$\left(C_c - \frac{\mu'\alpha\chi^2}{2fC_c^2} + \frac{\mu'\alpha}{2f} - C_e\right) + \frac{\mu\alpha}{2} - \frac{\mu'\alpha}{2}\frac{1-\beta}{\beta} - f\frac{(1-\beta)}{\beta} \times \left(\frac{\mu'\alpha\chi^2}{2fC_c^2} - \frac{\mu'\alpha}{2f}\right) = 0 \tag{A.7}$$

Multiplying all terms in Eq. (A.7) by C_c^2 gives

$$C_c^3 - \frac{\mu'\alpha\chi^2}{2f} + C_c^2\left(\frac{\mu'\alpha}{2f} - C_e\right) + \left(\frac{\mu\alpha}{2} - \frac{\mu'\alpha}{2}\frac{1-\beta}{\beta}\right)C_c^2 - f\frac{(1-\beta)}{\beta}\left(\frac{\mu'\alpha\chi^2}{2f} - \frac{\mu'\alpha}{2f}C_c^2\right) = 0 \tag{A.8}$$

Rearranging Eq. (A.8) gives

$$C_c^3 + C_c^2\left[\frac{\mu'\alpha}{2f} - C_e + \frac{\mu\alpha}{2} - \frac{\mu'\alpha}{2}\frac{1-\beta}{\beta} + f\frac{(1-\beta)}{\beta}\frac{\mu'\alpha}{2f}\right] - f\frac{(1-\beta)}{\beta}\left(\frac{\mu'\alpha\chi^2}{2f}\right) - \frac{\mu'\alpha\chi^2}{2f} = 0 \tag{A.9}$$

Eq. (A.9) reduces to

$$C_c^3 + C_c^2\left[\frac{\mu'\alpha}{2f} - C_e + \frac{\mu\alpha}{2}\right] - \frac{\mu'\alpha\chi^2}{2f\beta}(\beta + f(1-\beta)) = 0 \tag{A.10}$$

Note that in Eqs. (A.5) and (A.10), μ' is always divided by f. The parameter f appears in only one other place, where it multiplies $(1-\beta)$ in Eq. (A.10). The sensitivity of the quotient $\frac{\beta+f(1-\beta)}{\beta}$ to the value assigned to f is negatively correlated with β for β in the range zero to one. If respiration is ignored, Eq. (A.10) is identical to Eq. (10).

In the case of model 2, we begin with Eq. (A.3) but set $C_i = C_e$. This leads to

$$2P'B_2(C_c - C_e) + \mu' CB_2 - \frac{B_3\mu' CK_m}{C_c^2} = 0 \tag{A.11}$$

Dividing all terms in Eq. (A.11) by $2P'B_2$ gives

$$C_c - C_e + \frac{\mu'\alpha}{2f} - \frac{\chi^2\mu'\alpha}{2fC_c^2} = 0 \tag{A.12}$$

Rearranging Eq. (A.12) gives

$$C_c^3 + \left(\frac{\mu'\alpha}{2f} - C_e\right)C_c^2 - \frac{\chi^2\mu'\alpha}{2f} = 0 \tag{A.13}$$

Eq. (A.13) is identical to Eq. (14) when $\mu = \mu'$. Note that in Eq. (A.13) μ' and f always appear in the ratio μ'/f.

We now proceed to the derivation of the analogue of Eq. (21), again assuming that respired carbon is returned to the cytosol. The respired carbon is assumed to have the same isotopic signature as the fixed carbon, i.e., $\delta_b - \varepsilon_{fix}$. Given these assumptions, the analogues of Eqs. (19) and (20) are

$$(P(C_i - C_e) + \mu C)(\delta_{source} - \varepsilon_t) + C_eP(\delta_c - \varepsilon_t) + C_cP'(\delta_b - \varepsilon_t) + (\mu' - \mu)C(\delta_b - \varepsilon_{fix}) = C_iP'(\delta_a - \varepsilon_t) + (P'(C_c - C_i) + \mu' C)(\delta_a - \varepsilon_t) + C_iP(\delta_a - \varepsilon_t) \tag{A.14}$$

$$C_iP'(\delta_a - \varepsilon_t) + (P'(C_c - C_i) + \mu' C)(\delta_a - \varepsilon_t) = C_cP'(\delta_b - \varepsilon_t) + \mu' C(\delta_b - \varepsilon_{fix}) \tag{A.15}$$

The last term on the left-hand side of Eq. (A.14) accounts for the input of respired carbon to the cytosol. Other terms are as described for Eqs. (19) and (20), but with the caveat that the photosynthetic rate is now $\mu' C$, not μC. Note that this does not affect the term describing uptake from the external medium, since the cycling is internal to the cell.

To derive an expression for ε_p, we first solve Eq. (A.15) for δ_b:

$$\begin{aligned}\delta_b(C_cP' + \mu' C) &= C_iP'(\delta_a - \varepsilon_t) + (P'(C_c - C_i) + \mu' C)(\delta_a - \varepsilon_t) + C_cP'\varepsilon_t + \mu' C\varepsilon_{fix} \\ &= P'C_c\delta_a + \mu' C(\varepsilon_{fix} + \delta_a - \varepsilon_t)\end{aligned} \tag{A.16}$$

Solving Eq. (A.16) for δ_b gives

$$\begin{aligned}\delta_b &= \frac{P'C_c\delta_a + \mu' C(\delta_a - \varepsilon_t + \varepsilon_{fix})}{P'C_c + \mu' C} \\ &= \delta_a + \frac{\mu' C(\varepsilon_{fix} - \varepsilon_t)}{P'C_c + \mu' C}\end{aligned} \tag{A.17}$$

Given this expression for δ_b, we note that

$$\begin{aligned}\delta_b - \varepsilon_{fix} &= \delta_a - \left(\frac{P'C_c}{P'C_c + \mu' C}\right)\varepsilon_{fix} - \frac{\mu' C\varepsilon_t}{P'C_c + \mu' C} \\ &= \delta_a - \varepsilon_t + \frac{P'C_c}{P'C_c + \mu' C}(\varepsilon_t - \varepsilon_{fix})\end{aligned} \tag{A.18}$$

We now define the dimensionless quantity $\Theta_b = \frac{P'C_c}{P'C_c + \mu' C}$ and conclude that

$$\delta_b - \varepsilon_{fix} = \delta_a - \varepsilon_t + \Theta_b(\varepsilon_t - \varepsilon_{fix}) \tag{A.19}$$

We note that by definition $\delta_b - \varepsilon_{fix} = \delta_c - \varepsilon_p$. Given this definition, it follows from Eq. (A.19) that

$$\varepsilon_p = -\delta_a + \varepsilon_t + \delta_c - \Theta_b(\varepsilon_t - \varepsilon_{fix}) \tag{A.20}$$

Substituting the right-hand side of Eq. (A.17) for the first δ_b on the left-hand side of Eq. (A.14) we obtain

$$(P(C_i - C_e) + \mu C)(\delta_{source} - \varepsilon_t) + C_eP(\delta_c - \varepsilon_t) + \Theta_b\mu' C(\varepsilon_{fix} - \varepsilon_t) + (\mu' - \mu)C(\delta_b - \varepsilon_{fix}) = (\delta_a - \varepsilon_t) \times (C_iP' + P'(C_c - C_i) + \mu' C + C_iP - C_cP') = (\delta_a - \varepsilon_t)(\mu' C + C_iP) \tag{A.21}$$

Now substituting the right-hand side of Eq. (A.19) for $\delta_b - \varepsilon_{fix}$ in (A.21) gives

$$(P(C_i - C - e) + \mu C)(\delta_{source} - \varepsilon_t) + C_e P(\delta_c - \varepsilon_t) + \Theta_b \mu C(\varepsilon_{fix} - \varepsilon_t) = (\delta_a - \varepsilon_t)(\mu C + C_i P) \quad (A.22)$$

Rearranging Eq. (A.22) gives

$$\frac{(P(C_i - C_e) + \mu C)(\delta_{source} - \varepsilon_t) + C_e P(\delta_c - \varepsilon_t) + \Theta_b \mu C(\varepsilon_{fix} - \varepsilon_t)}{(\mu C + C_i P)} = \delta_a - \varepsilon_t \quad (A.23)$$

It follows from Eq. (A.20) that

$$\varepsilon_p = -\delta_a + \varepsilon_t + \delta_c - \Theta_b(\varepsilon_t - \varepsilon_{fix}) = \delta_c - \Theta_b(\varepsilon_t - \varepsilon_{fix}) - \frac{(P(C_i - C_e) + \mu C)(\delta_{source} - \varepsilon_t) + C_e P(\delta_c - \varepsilon_t) + \Theta_b \mu C(\varepsilon_{fix} - \varepsilon_t)}{(\mu C + C_i P)} \quad (A.24)$$

Now define $\Theta_a = \frac{C_i P}{\mu C + C_i P}$ and $\gamma = \frac{P(C_i - C_e) + \mu C}{\mu C}$

Collecting like terms, it follows that

$$\varepsilon_p = (\delta_c - \delta_{source})\gamma(1 - \Theta_a) + \Theta_a \Theta_b(\varepsilon_{fix} - \varepsilon_t) + \varepsilon_t \quad (A.25)$$

Eq. (A.25) is identical in form to Eq. (21), and the meanings of Θ_a, Θ_b, and γ are the same. Θ_a is the amount of CO_2 that leaks out of the cell as a fraction of gross uptake through the plasmalemma. Θ_b is the amount of CO_2 that leaks out of the chloroplast as a fraction of gross uptake by the chloroplast. And γ is the ratio of active transport through the plasmalemma to net growth rate. However, Θ_b in Eq. (A.25) equals $\frac{P' C_c}{P' C_c + \mu' C}$, whereas in equation 22 Θ_b is understood to equal $\frac{P' C_c}{P' C_c + \mu C}$. Note, however, that

$$\Theta_b = \frac{P' C}{P' C_c + \mu' C} = \frac{P C}{P C_c + \frac{\mu'}{f} C} \quad (A.26)$$

Since μ' and f do not appear in the definitions of Θ_a and γ, Eq. (A.25) involves μ' and f only in the ratio μ'/f.

References

Anderson, L.J., Maherali, H., Johnson, H.B., Polley, H.W., Jackson, R.B., 2001. Gas exchange and photosynthetic acclimation over subambient to elevated CO_2 in a C_3–C_4 grassland. *Global Change Biol.* **7** (6), 693–707.

Badger, M.R., 1987. The CO_2 concentrating mechanism in aquatic phototrophs*The Biochemistry of Plants: A Comprehensive Treatise*, vol. 10. Academic Press, pp. 132–218.

Badger, M.R., Andrews, T.J., Whitney, S.M., Ludwig, M., Yellowlees, D.C., Leggat, W., Price, G.D., 1998. The diversity and coevolution of Rubisco, plastids, pyrenoids, and chloroplast-based CO sub(2)-concentrating mechanisms in algae. *Can. J. Bot. Rev. Can. Bot.* **76** (6), 1052–1071.

Burkhardt, S., Amoroso, G., Riebesell, U., Sultemeyer, D., 2001. CO_2 and HCO_3^- uptake in marine diatoms acclimated to different CO_2 concentrations. *Limnol. Oceanogr.* **46** (6), 1378–1391.

Burkhardt, S., Riebesell, U., Zondervan, I., 1999. Effects of growth rate, CO_2 concentration, and cell size on the stable carbon isotope fractionation in marine phytoplankton. *Geochim. Cosmochim. Acta* **63** (22), 3729–3741.

Cassar, N. 2003. Carbon-concentrating mechanisms and β-carboxylation: their potential contribution to marine photosynthetic carbon isotope fractionation. Ph.D. dissertation, University of Hawaii.

Cassar, N., Laws, E.A., Popp, B.N., Bidigare, R.C., 2002. Sources of inorganic carbon for photosynthesis by marine diatoms. *Limnol. Oceanogr.* **47**, 1192–1197.

Colman, B., Huertas, I.E., Bhatti, S., Dason, J.S., 2002. The diversity of inorganic carbon acquisition mechanisms in eukaryotic microalgae. *Funct. Plant Biol.* **29**, 261–270.

Conte, M.H., Volkman, J.K., Eglinton, G., 1994. Lipid biomarkers of the haptophyta. In: Leadbeater, B.S.C. (Ed.), *The Haptophyta Algae*. Clarendon Press, pp. 351–377.

Descolas-Gros, C., Oriol, L., 1992. Variations in carboxylase activity in marine phytoplankton cultures. β-Carboxylation in carbon flux studies. *Mar. Ecol. Prog. Ser.* **85** (1-2), 163–169.

Falkowski, P.G., Katz, M.E., Knoll, A.H., Quigg, A., Raven, J.A., Schofield, O., Taylor, F.J.R., 2004. The evolution of modern eukaryotic phytoplankton. *Science (Wash.)* **305**, 354–360.

Fawley, M.W., 1984. Effects of light intensity and temperature interactions on growth characteristics of *Phaeodactylum tricornutum* (Bacillariophyceae). *J. Phycol.* **20**, 67–72.

Francois, R., Altabet, M.A., Goericke, R., McCorkle, D.C., Brunet, C., Poisson, A., 1993. Changes in the™ ^{13}C of surface water particulate organic matter across the subtropical convergence in the SW Indian ocean. *Global Biogeochem. Cycles* **7** (3), 627–644.

Goericke, R., Montoya, J.P., Fry, B., 1994. Physiology of isotopic fractionation in algae and cyanobacteria. In: Lajtha, K., Michener, R.H. (Eds.), *Stable Isotopes in Ecology and Environmental Science*. Blackwell Scientific Publications, pp. 187–221.

Johnston, A.M., 1991. The acquisition of inorganic carbon by marine macroalgae. *Can. J. Bot. Rev. Can. Bot.* **69** (5), 1123–1132.

Keller, K., Morel, F.M.M., 1999. A model of carbon isotopic fractionation and active carbon uptake in phytoplankton. *Mar. Ecol. Prog. Ser.* **182**, 295–298.

Lavergne, D., Bismuth, E., Champigny, M.L., 1979a. Physiological studies on two cultivars of *Pennisetum*: *P. americanum* 23 DB, a cultivated species, and *P. mollissimum*, a wild species. I. Photosythetic carbon metabolism. *Z. Pflphysiol.* **91**, 291–303.

Lavergne, D., Bismuth, E., Sarda, E., Champigny, M.L., 1979b. Physiological studies on two cultivars of *Pennisetum*: *P. americanum* 23 DB, a cultivated species, and *P. mollissimum*, a wild species. II. Effects of leaf age on biocehmical characteristics and activities of the enzymes associated with the photosynthetic carbon metabolism. *Z. Pflphysiol.* **93**, 159–170.

Laws, E., 1997. *Mathematical Methods for Oceanographers: An Introduction*. John Wiley & Sons.

Laws, E.A., Bidigare, R.R., Popp, B.N., 1997. Effect of growth rate and CO_2 concentration on carbon isotopic fractionation by the marine diatom *Phaeodactylum tricornutum*. *Limnol. Oceanogr.* **42** (7), 1552–1560.

Laws, E.A., Popp, B.N., Bidigare, R.R., Kennicutt, M.C., Macko, S.A., 1995. Dependence of phytoplankton carbon isotopic composition on growth rate and $[CO_2]_{aq}$: theoretical considerations and experimental results. *Geochim. Cosmochim. Acta* **59** (6), 1131–1138.

Laws, E.A., Popp, B.N., Cassar, N., Tanimoto, J., 2002. ^{13}C discrimination patterns in oceanic phytoplankton: likely influence of CO_2 concentrating mechanisms, and implications for palaeoreconstructions. *Funct. Plant Biol.* **29** (2-3), 323–333.

Martin, W., Rujan, T., Richly, E., Hansen, A., Cornelsen, S., Lins, T., Leister, D., Stoebe, B., Hasegawa, M., Penny, D., 2002. Evolutionary analysis of *Arabidopsis*, cyanobacterial, and chloroplast genomes reveals plastid phylogeny and thousands of cyanobacterial genes in the nucleus. *Proc. Natl. Acad. Sci. USA* **99** (19), 12246–12251.

Pagani, M., Zachos, J.C., Freeman, K.H., Tipple, B., Bohaty, S., 2005. Marked decline in atmospheric carbon dioxide concentrations during the Paleogene. *Science (NY)* **309**, 600–603.

Popp, B.N., Laws, E.A., Bidigare, R.R., Dore, J., Hanson, K.L., Wakeham, S.G., 1998. The effect of phytoplankton cell geometry on carbon isotopic fractionation. *Geochim. Cosmochim. Acta* **62**, 69–77.

Popp, B.N., Parekh, P., Tilbrook, B., Bidigare, R.R., Laws, E.A., 1997. Organic carbon delta ^{13}C variations in sedimentary rocks as chemostratigraphic and paleoenvironmental tools. *Palaeogeogr. Palaeoclimatol. Palaeoecol.* **132** (1-4), 119–132.

Rau, G.H., Riebesell, U., Wolf-Gladrow, D., 1997. CO_{2aq}-dependent photosynthetic ^{13}C fractionation in the ocean: a model versus measurements. *Global Biogeochem. Cycles* **11** (2), 267–278.

Raven, J.A., 1997. Inorganic carbon acquisition by marine autotrophs. *Adv. Bot. Res.* **27**, 85–209.

Raven, J.A., Brown, K., Mackay, M., Beardall, J., Giordano, M., Granuum, E., Leegood, R.C., Kilminster, K., Walker, D.I., 2005. Iron, nitrogen, phosphorus and zinc cycling and consequences for primary productivity in the oceans. In: Gadd, G.M., Semple, K.T., Lappin-Scott, H.M. (Eds.), *Micro-Organisms and Earth Systems—Advances in Geomicrobiology*. Cambridge University Press, pp. 247–272.

Reinfelder, J.R., Kraepiel, A.M.L., Morel, F.M.M., 2000. Unicellular C_4 photosynthesis in a marine diatom. *Nature* **407** (6807), 996–999.

Reinfelder, J.R., Milligan, A.J., Morel, F.M.M., 2004. The role of the C_4 pathway in carbon accumulation and fixation in a marine diatom. *Plant Physiol.* **135**, 1–6.

Riebesell, U., Burkhardt, S., Dauelsberg, A., Kroon, B., 2000. Carbon isotope fractionation by a marine diatom: dependence on the growth-rate-limiting resource. *Mar. Ecol. Prog. Ser.* **193**, 295–303.

Sage, R.F., 1990. A model describing the regulation of Ribulose-1,5-bisphosphate carboxylase, electron trasnport, and triose phosphate use in response to light intensity and CO_2 in C_3 plants. *Plant Physiol.* **94**, 1728–1734.

Sage, R.F., 1994. Acclimation of photosynthesis to increasing atmospheric CO_2—the gas-exchange perspective. *Photosynth. Res.* **39** (3), 351–368.

Sharkey, T.D., Berry, J.A., 1985. Carbon isotope fractionation of algae as influenced by an inducible CO_2 concentrating mechanism. In: Lucas, W.J., Berry, J.A. (Eds.), *Inorganic Carbon Uptake by Aquatic Photosynthetic Organisms*. American Society of Plant Physiologists, pp. 389–399.

Tanaka, Y., Nakatsuma, D., Harada, H., Ishida, M., Matsuda, Y., 2005. Localization of soluble b-carbonic anhydrase in the marine diatom *Phaeodactylum tricornutum*. Sorting to the chloroplast and cluster formation on the girdle lamellae. *Plant Physiol.* **138**, 207–217.

Terry, K.L., Hirata, J., Laws, E.A., 1983. Light-limited growth of two strains of the marine diatom *Phaeodactylum tricornutum* Bohlin: chemical composition, carbon partitioning and the diel periodicity of physiological processes. *J. Exp. Mar. Biol. Ecol.* **68** (3), 209–227.

Thoms, S., Pahlow, M., Wolf-Gladrow, D.A., 2001. Model of the carbon concentrating mechanism in chloroplasts of eukaryotic algae. *J. Theor. Biol.* **208**, 295–313.

Volkman, J.K., Barrett, S.M., Blackburn, S.I., Sikes, E.L., 1995. Alkenones in *Gephyrocapsa oceanica*: implications for studies of paleoclimate. *Geochim. Cosmochim. Acta* **59**, 513–520.

Volkman, J.K., Eglinton, G., Corner, E.D.S., Forsberg, T.E.V., 1980a. Long chain alkenes and alkenones in the marine coccolithophorid *Emiliania huxleyi*. *Phytochemistry*, 2619–2622.

Volkman, J.K., Eglinton, G., Corner, E.D.S., Sargent, J.R., 1980b. Novel unsaturated straight chain C37–C39 methyl and ethyl ketones in marine sediments and a coccolithosphore *Emiliania huxleyi*. In: Maxwell, J.R. (Ed.), *Advances in Organic Geochemistry*. Pergamon Press, pp. 219–228.